

---

# ACTIVE LABEL CLEANING FOR RELIABLE DETECTION OF ELECTRON DENSE DEPOSITS IN TRANSMISSION ELECTRON MICROSCOPY IMAGES

---

**Jieyun Tan\***

School of Biomedical Engineering  
Southern Medical University  
Guangzhou, China

**Shuo Liu\***

School of Biomedical Engineering  
Southern Medical University  
Guangzhou, China

**Guibin Zhang\***

School of Biomedical Engineering  
Southern Medical University  
Guangzhou, China

**Ziqi Li**

College of Letters and Science  
University of Wisconsin-Madison  
Madison, USA

**Jian Geng**

School of Basic Medical Sciences  
Southern Medical University  
Guangzhou, China

**Lei Zhang**

Department of Nephrology  
Nanfang Hospital, Southern Medical University  
Guangzhou, China

**Lei Cao†**

School of Biomedical Engineering  
Southern Medical University  
Guangzhou, China  
caolei@smu.edu.cn

February 6, 2026

## ABSTRACT

Electron dense deposits (EDD) provide crucial diagnostic references for glomerular disease. However, manual identification of EDD is labor-intensive and variable across observers, underscoring the need for automated and reliable image analysis tools. Yet, the accuracy of deep learning-based detection remains constrained by the lack of large, high-quality labeled datasets. Although crowdsourcing can lower annotation costs, it inevitably introduces label noise. To address this, we propose a novel active label cleaning method to effectively reduce label noise and improve data quality. We employ active learning to select the most valuable noisy samples for re-annotation by pathologists, constructing high-accuracy cleaning models at a minimal cost. These models are then utilized to perform a noise-graded correction on the crowdsourced labels. A core component, the Label Selection Module, leverages the inconsistency between crowdsourced labels and model predictions to achieve both image-level sample selection and instance-level noise grading. Experimental results show that our method achieves 67.18% AP<sub>50</sub> on the private dataset, an 18.83% improvement over noisy training. This performance reaches 95.79% of that achieved with full pathologist annotation while reducing annotation cost by 73.30%, ultimately delivering superior detection performance over existing noisy training methods at a lower cost. These results demonstrate that the proposed active label cleaning method provides a practical and efficient solution for building reliable medical AI systems under limited expert annotation resources.

**Keywords** Electron dense deposits, Object detection, Label cleaning, Active learning

---

\*These authors contributed equally.

†Corresponding author: Lei Cao (caolei@smu.edu.cn).

## 1 Introduction

Electron dense deposits (EDD) are immune complexes visible in transmission electron microscopy (TEM) images which can provide crucial diagnostic references for glomerular disease [1, 2]. Recent progress in deep learning leads to substantially improvements in automatic detection of EDD [3, 4], which has the potential to facilitate pathologists' diagnostic work. Nevertheless, due to the scarcity of labeled large-scale datasets, the model's detection accuracy does not achieve the requisite for clinical application. There are two main factors contributing to EDD annotation scarcity. Firstly, medical image annotation requires professional expertise and typically involves the collaboration of three or more experts to ensure the reliability [5]. Secondly, the annotation process for EDD in TEM images is costly and time-consuming because of their large quantity, diverse morphology, and similarity to other ultra-structures in terms of shape and grayscale distribution.

In the medical field, crowdsourcing (data labeling through non-expert annotators) is an effective method to addresses insufficient labeling [6], but it inevitably introduces noise [7]. Hence, research on effective methods to reduce the influences of noise within datasets is crucial [8]. Among existing methods, noise-robust learning [9, 10] improves efficiency by directly training models on noisy data without label correction. However, it requires substantial training data to cover various types and levels of noises to make up accuracy loss, which is inappropriate for data-limited clinical scenarios. In contrast, label cleaning selects samples (i.e., images) and corrects noisy labels by establishing a cleaning model [11, 12], which theoretically has higher detection accuracy. However, if the cleaning model is trained solely on noisy data, its training signals (e.g., loss, gradient) cannot reliably reflect true noise level, leading to lower accuracy in sample selection and label correction. Moreover, constrained by the training algorithm and data, exclusively relying on automatically correction of noisy labels via the cleaning model presents a latent risk of learning the bias in the noise, which may further amplify label noise [13].

To mitigate label noise and improve data quality, (1) we designed a two-step process to construct high-accuracy cleaning models that perform label correction using only datasets labeled by pathologists. Clean label acquisition is costly, so (2) we introduce an active learning method to perform image-level sample selection in the first step, maximizing the effectiveness of training data while controlling annotation cost. We use the proposed Label Selection Module (LSM) to analyze the inconsistency between crowdsourced labels and model predictions, which helps us to select the most valuable samples for labeling. In the second step, (3) we perform instance-level label correction (where each instance corresponds to one label) based on the LSM's discrimination results: labels with simple noise are automatically corrected by the model, while those with complex noise are assigned to pathologists for review. This approach significantly reduces annotation cost while improving the reliability of the corrections.

The remainder of this paper is structured as follows: Section 2 introduces related works on object detection with noisy label and active learning; Section 3 presents a detailed description of the private dataset and the proposed method; Section 4 reports the experimental settings and results; and Section 5 concludes the paper.

## 2 Related work

### 2.1 Object detection with noisy label

In object detection tasks with noisy label, the smallest unit to measure noise level is the bounding box(i.e., instance or label). Thus, the noise types include not only classification error, but also background noise, miss noise, location noise, etc. [14], as illustrated in Figure 1. In current research, some methods aim to improve the robustness of the model on data with noisy label. For example, NOTE-RCNN [9] avoids involving complex noisy labels in training via semi-supervised methods, while OA-MIL [10] designs robust training strategies for incomplete and imprecise bounding boxes. However, these methods only enhance the model's noise tolerance at the algorithmic level but are unable to eliminate the noise, and the residual label noise still limits the achievable accuracy, especially in high-precision tasks such as medical image analysis.

Other approaches leverage models trained on noisy data for sample selection and label correction, thereby eliminating label noise. For example, CA-BBC [11] corrects location errors in noisy labels using gradient information and adjusts classification errors by model predictions, yet updates all labels indiscriminately. Mao et al. [12] re-annotate those noisy labels which significantly differ from previous predictions in each epoch. Although such selection-based corrections can reduce obvious errors, methods that depend primarily on a single model's predictions remain vulnerable when model reliability degrades under high noise. This dependency limits the extent to which automatic correction can approach expert-level annotations in noisy scenarios.

## 2.2 Active learning

Active learning aims to minimize annotation cost by selecting the most informative training samples for improving model accuracy [15, 16]. In object detection tasks, representative works include LT/C and LS+C [17], which assess image information for sample selection by calculating the tightness and stability of instances, respectively. Meanwhile, CALD [18] selects samples by analyzing the inconsistency of predictions before and after data augmentation. More recently, OSAL-ND [19] first selects candidate samples through prototypes and then queries the most uncertain samples for re-annotation. For task-unaware active learning methods, VAAL [20] and LLAL [21] leverage image features or training signals to select samples by calculating the latent features or losses.

In addition, active label cleaning (ALC) has attracted wide attention as an essential application of active learning for data with noisy label, particularly for medical image processing [13]. For example, Khanal et al. [22] propose a two-phase approach combining noisy label learning and active label cleaning to improve the robustness of medical image classification under limited budgets. However, to our knowledge, ALC methods that explicitly target instance-level label noise and the spatial complexity of detection remain relatively underexplored.

## 3 Methods

### 3.1 Dataset

This study was a retrospective study. The private dataset was collected from a certified medical laboratory center, all data has been anonymized, personal information excluded. A total of 1112 glomerular TEM images ( $2,048 \times 2,048$ ) were acquired from 202 patients with membranous nephropathy who underwent renal biopsy, each image contained one or more EDD: 131 images were randomly selected for validation, 234 for testing, and the rest for training. The annotators include 5 medical students with basic training, serving as crowd, and 3 senior pathologists with over a decade of experience. Crowd-annotated labels may contain noise, whereas pathologist-annotated labels are considered clean. We conducted a comparative analysis of these two types of labels to effectively clean the noise data, as shown in Figure 1. Meanwhile, Figure 2 shows an example of Bib noise, which occurs when blurred EDD edges cause crowd annotators to box multiple instances together.

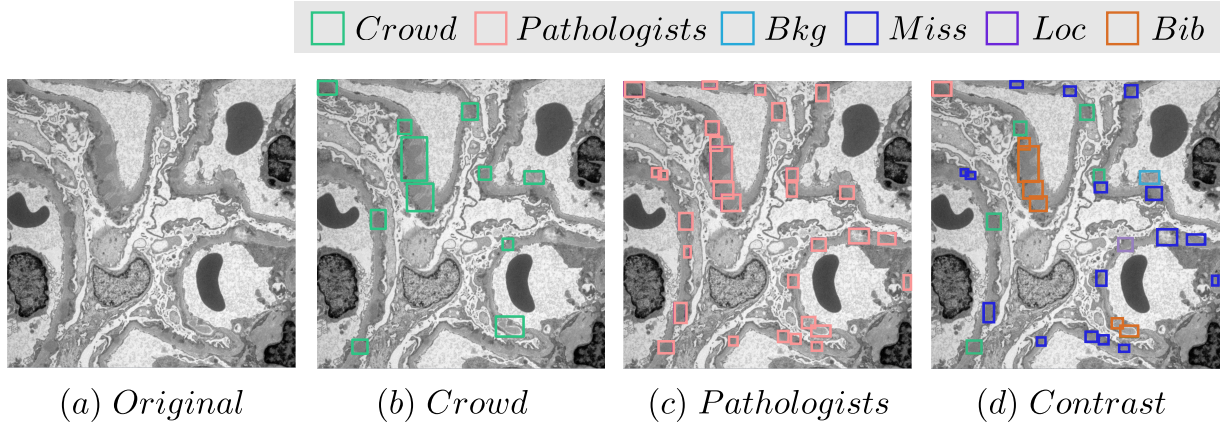


Figure 1: Classification of labels. (a) Original TEM images; (b) Crowdsourced labels with noise (green bounding boxes); (c) Pathologists-corrected clean labels (pink bounding boxes); (d) Comparison of annotation differences, categorized into: Bkg (background noise, background misclassified as foreground, light blue), Miss (miss noise, ground truth missed by annotators, deep blue), Loc (location noise, boxes incorrectly localized, purple), and Bib (box-in-box noise, boxes incorrectly nested, orange).

### 3.2 Framework Overview

The proposed method involves two steps: Step 1 is Active learning, which is used to train cleaning models. Step 2 is Label correction, which corrects noisy labels using the cleaning models constructed in Step 1. Both steps rely on the Label Selection Module. The entire process is illustrated in Figure 3.

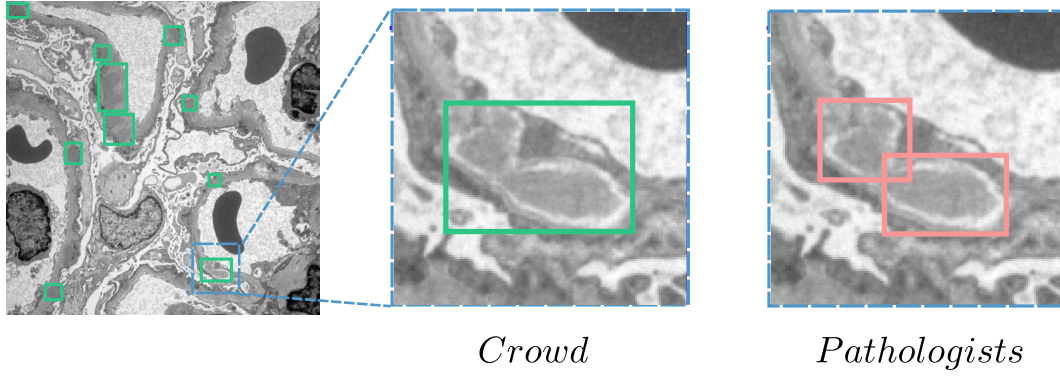
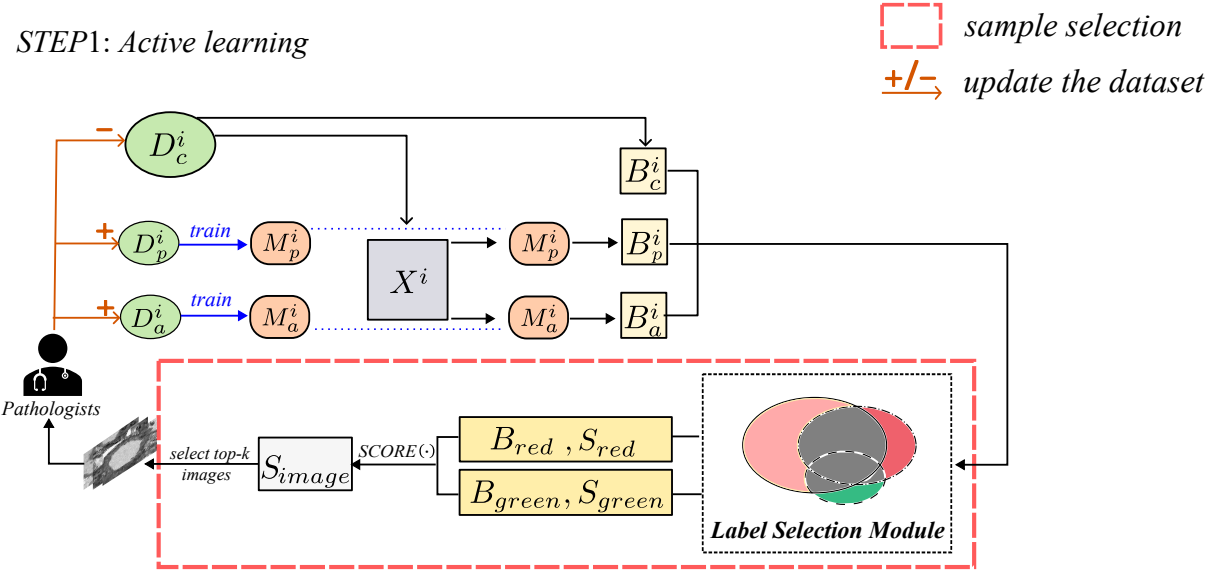


Figure 2: Bib (Box-in-Box) Noise in crowdsourced labels. Blurred EDD edges in the dataset led crowd annotators to occasionally include multiple EDD within a single bounding box. While pathologists avoid this error, it reflects a common localization artifact in crowdsourced label.



*STEP2: Label correction*

Legend: □ noise graded correction

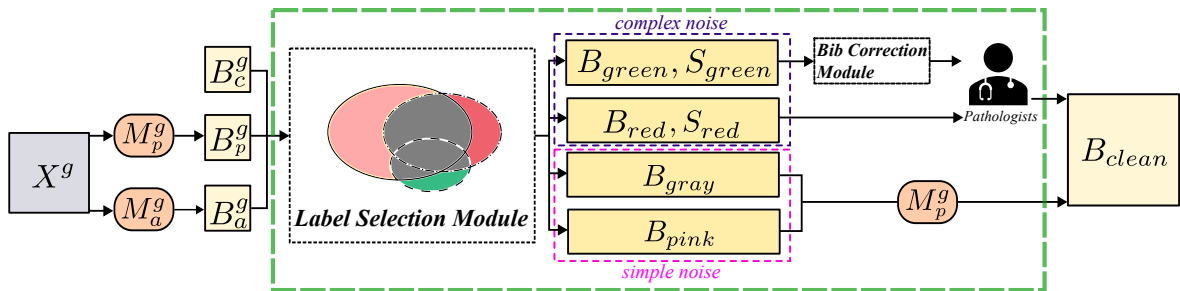


Figure 3: Overview of the proposed method.

### 3.3 Initialization

As illustrated in Figure 3,  $X$  represents the entire set of images. Initially ( $i = 0$ ),  $X^0$  (a subset of images) is randomly selected from  $X$  and provided to pathologists for annotation, resulting in the initial clean dataset  $D_p^0$ . The corresponding crowdsourced dataset is  $D_c^0$ . Next, labels corresponding to EDD that are validated by both crowd and pathologists are selected to construct the consensus dataset  $D_a^0$ . After obtaining these initial datasets, two architecturally identical models are initialized. Based on their respective training datasets, they are denoted as  $M_p^0$  and  $M_a^0$ . The former is a cleaning model trained on the clean dataset, while the latter is trained on the consensus dataset.

### 3.4 Label Selection Module

As illustrated in Figure 4, the primary function of the Label Selection Module (LSM) in the  $i$ -th iteration is to identify potential noisy labels by comparing crowdsourced labels with the predictions of two models ( $M_p^i$  and  $M_a^i$ ). It then classifies these labels based on their degree of inconsistency and assigns each a quantified score, thereby providing a basis for following active learning and label cleaning. Specifically,  $B_a^i$  represents the prediction results of  $M_a^i$ . Due to the incompleteness of training data, it may contain Miss noise. In contrast,  $B_p^i$  represents the prediction results of  $M_p^i$  trained using all available clean labels. While  $M_p^i$  can detect more EDD, it is more sensitive to abnormal cases because its training data includes more anomalous instances, particularly atypical EDD. This heightened sensitivity, especially pronounced in early stages with limited training data where the model may overfit, can lead to a higher propensity for false positives (Bkg noise) in its predictions, though this effect attenuates as training data increases.

In this module, we categorize label regions as follows:

- **Red Region ( $B_{red}$ )**: This region indicates labels in the detection results  $M_a^i$  that do not consent with the results from  $M_p^i$  or the crowdsourced labels  $B_c^i$ . These labels show significant inconsistency and usually contain substantial noise.
- **Pink Region ( $B_{pink}$ )**: This region represents labels that only appear in the detection results of  $M_p^i$ , potentially due to omissions by crowd. As  $M_p^i$  is trained on high-quality data, it can reliably identify these missing EDD annotations, thereby correcting the Miss noise contained within this region.
- **Green Region ( $B_{green}$ )**: This region represents labels that only appear in the crowdsourced labels  $B_c^i$ , probably incorrectly annotated by crowd annotators. These labels are often associated with samples that are challenging to identify, may contain complex noise including Bkg, Loc, Bib noise.
- **Grey Region ( $B_{gray}$ )**: This region indicates labels with high consistency between  $B_c^i$ ,  $B_p^i$ , and  $B_a^i$ , specifically when the Intersection over Union (IoU) of instances in any two sets is greater than 0.5. These labels correspond to EDD that the model can accurately identify, typically containing no noise or only a small amount of noise.

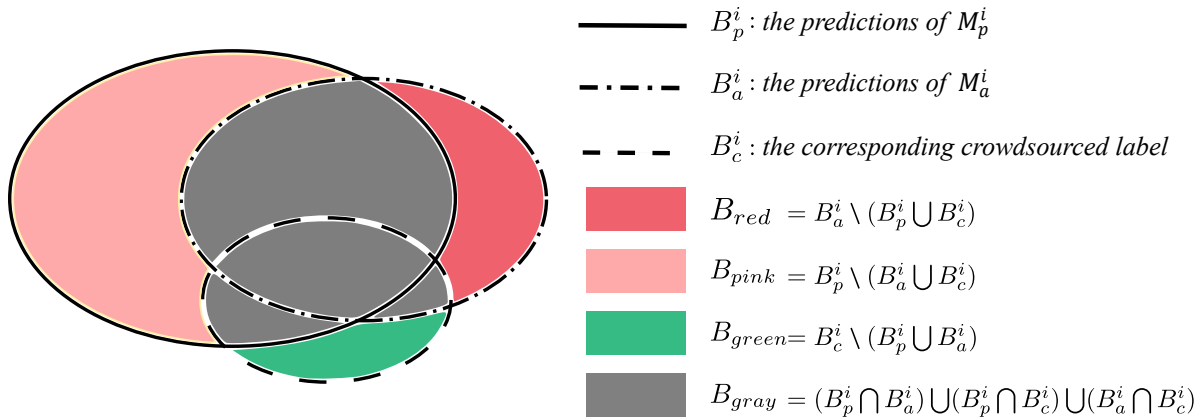


Figure 4: Label Selection Module diagram.

We prioritize complex noisy labels ( $B_{red}$  and  $B_{green}$ ) over the simple noisy labels ( $B_{gray}$  and  $B_{pink}$ ) that can be automatically corrected. To select the most valuable images for active learning, we need to assess the inconsistency of labels within each image. Specifically, for each label in  $B_{red}$ , we use the confidence score from  $M_a^i$ 's prediction as the evaluation score, yielding the score set  $S_{red}$  corresponding to  $B_{red}$ . For each label in  $B_{green}$ , we use the confidence score of the bounding box with the highest IoU from  $M_p^i$ 's prediction as the evaluation score, yielding the score set  $S_{green}$  corresponding to  $B_{green}$ .

### 3.5 Step 1: Active learning

Figure 3 reveals that Step 1 iteratively select and annotate samples using active learning to construct the cleaning models. In the  $i$ -th iteration, the consensus dataset  $D_a^i$  is built using the clean dataset  $D_p^i$  and the corresponding crowdsourced dataset  $D_c^i$ . Let  $X^i = X^{i-1} \cup A^i$  (where  $i \geq 1$ ) denote the current accumulated image set, with  $X^0$  as the initial set and  $A^i$  representing newly added images in the  $i$ -th iteration. For each image in  $X^i$ , if there exists a label  $b_p$  from  $D_p^i$  and a label  $b_c$  from  $D_c^i$  satisfy Equation (1) (where  $\delta$  is the threshold), the consensus labels  $B_p$  (all matching  $b_p$  instances) are added to  $D_a^{i-1}$  to form  $D_a^i$ .

$$D_a^i \leftarrow D_a^{i-1} \cup \{(x, B_p) \mid x \in X^i, B_p = \{b_p \in D_p^i \mid \exists b_c \in D_c^i : b_c \cap b_p / b_p > \delta\}\} \quad (1)$$

Subsequently,  $M_p^i$  and  $M_a^i$ , are trained using  $D_p^i$  and  $D_a^i$ , respectively. They detect EDD in the remaining image set  $X \setminus X^i$ , producing results  $B_p^i$  and  $B_a^i$ . The LSM then analyzes the inconsistencies among  $B_p^i$ ,  $B_a^i$  and the corresponding crowdsourced labels  $B_c^i$ , selecting complex noisy label sets  $B_{\text{red}}$  and  $B_{\text{green}}$ , along with their evaluation score sets  $S_{\text{red}}$  and  $S_{\text{green}}$ . The image scores are then aggregated to select samples. For the  $j$ -th image  $x_j \in X \setminus X^i$ , an aggregation function  $SCORE(\cdot)$  computes its inconsistency score by summing instance-level evaluation scores from  $S_{\text{red}}$  and  $S_{\text{green}}$  associated with labels within  $x_j$ .

$$SCORE(x_j) = \sum_{l \in B_{\text{red}} \cup B_{\text{green}}} (s_{\text{red}}^l + s_{\text{green}}^l) \quad (2)$$

where  $s_{\text{red}}^l$  and  $s_{\text{green}}^l$  denote the instance-level scores for label  $l$  in  $S_{\text{red}}$  and  $S_{\text{green}}$ , respectively.

After quantifying label inconsistency, the top- $k$  most inconsistent images (indicating highly noisy labels or difficult-to-identify EDD) are selected for pathologist review. Corrected labels are then used to expand  $D_p^i$ , generating the updated clean dataset  $D_p^{i+1}$ . Simultaneously, the corresponding noisy labels are removed from  $D_c^i$  to produce  $D_c^{i+1}$ , and  $D_a^{i+1}$  is expanded following Equation (1). This process iterates until the stopping condition is met at the  $g$ -th iteration, yielding final cleaning models  $M_p^g$  and  $M_a^g$  for label correction.

### 3.6 Step 2: Label correction

Figure 3 shows that Step 2 performs instance-level noise-graded correction on the remaining noisy labels in  $D_c^g$ , leveraging the cleaning models  $M_p^g$  and  $M_a^g$  constructed in Step 1. First, we apply  $M_p^g$  and  $M_a^g$  to detect EDD in the remaining image set  $X \setminus X^g$ , producing results  $B_p^g$  and  $B_a^g$ . These results, along with the corresponding noisy labels  $B_c^g$ , are fed into the LSM, which classifies the labels into four categories:  $B_{\text{gray}}$ ,  $B_{\text{pink}}$ ,  $B_{\text{red}}$  and  $B_{\text{green}}$ .

For labels with simple noise ( $B_{\text{gray}}$  and  $B_{\text{pink}}$ ), we automatically correct them by adding missing labels or replacing incorrect ones in  $D_c^g$  with the predictions  $B_p^g$  from  $M_p^g$ , as  $M_p^g$  was trained on the fully clean dataset and demonstrates superior detection performance to  $M_a^g$ . Labels with complex noise ( $B_{\text{red}}$  and  $B_{\text{green}}$ ) are submitted to pathologists for manual correction, with  $B_p^g$  and  $B_a^g$  provided as reference suggestions.

Notably, the LSM is unable to identify Bib noise in some labels within  $B_{\text{green}}$ . Since such noise can be auto-corrected to reduce pathologists' time. Inspired by [23], we developed a Bib Correction Module before manual review. For each label  $b_{\text{green}} \in B_{\text{green}}$ , if there exists  $b^*$  (where  $b^* \in B_{\text{gray}} \cup B_{\text{pink}} \cup B_{\text{red}}$ ) satisfying Equation (3) (where  $\gamma$  is the threshold),  $b_{\text{green}}$  is identified as Bib noise and removed, while  $b^*$  is retained as the correct label.

$$B_{\text{green}} \leftarrow B_{\text{green}} \setminus \left\{ b_{\text{green}} \mid \exists b^* \in B_p^g \vee b^* \in B_a^g : \frac{b^* \cap b_{\text{green}}}{b^*} > \gamma \right\} \quad (3)$$

The final clean labels  $B_{\text{clean}}$  are generated by combining auto-corrected and manually corrected labels, thereby completing the noise-graded correction for remaining noisy labels in  $D_c^g$ .

## 4 Experimental results

### 4.1 Experimental settings

All experiments were conducted on an RTX 3090 GPU using MMDETECTION [24]. We employed FASTER R-CNN [25] with a RESNET-50 (pre-trained on ImageNet) + FPN backbone, trained for 36 epochs with batch size of 4. The

SGD optimizer was configured with a learning rate of 0.01, momentum of 0.9, and weight decay of  $1 \times 10^{-4}$ . To enhance model robustness, data augmentation was applied using random flipping, rotation, scaling, and clipping. In Step 1, active learning began with 40 randomly selected images ( $|X^0| = 40$ ). The consensus dataset  $D_a^i$  was constructed using a threshold  $\delta = 0.5$ , with 4 iterations ( $g = 4$ ) selecting 40 samples ( $k = 40$ ) per iteration, culminating in 200 samples (26.77% of total) for final models training. In Step 2, the Bib Correction Module’s threshold  $\gamma$  was set to 0.8. We evaluated model performance using  $AP_{50}$  and assessed label cleaning effectiveness through TIDE [26] analysis of three noise types. The annotation cost ratio between crowd and pathologist efforts was maintained at 1 : 10. All experiments were repeated three times with averaged results reported.

## 4.2 Comparison Results

Table 1 shows the evaluation results of our proposed method on the private dataset, which was retrained  $M_p$  using  $D_p^g$  after Step 2, and evaluated on the test set. Compared with other methods, our approach achieved the best performance with an  $AP_{50}$  of 67.18%, demonstrating an 18.83% improvement over the uncleaned baseline of Noisy Training and reaching 95.79% of the performance of the Clean Training (a model trained on pathologist-annotated data). This indicates that our method enables robust training in practical applications. Furthermore, TIDE analysis reveals that our approach significantly reduces all three types of noise.

Table 1: Comparison of different noise treatment methods on private dataset.

Method	$AP_{50}(\%) \uparrow$	TIDE Analysis			Budget(%) $\downarrow$
		Bkg $\downarrow$	Miss $\downarrow$	Loc $\downarrow$	
Noisy Training	48.35	5.34	15.94	17.05	3.52
OA-MIL	49.90(+1.55)	3.99(-1.35)	14.77(-1.17)	20.90(+3.85)	<b>3.52</b>
Mao	56.23(+7.88)	4.92(-0.42)	16.34(+0.40)	13.63(-3.42)	<b>3.52</b>
ALC	63.67(+15.32)	4.32(-1.02)	11.77(-4.17)	12.65(-4.40)	26.71(+23.19)
Ours (Random)	64.07(+15.72)	4.33(-1.01)	12.06(-3.88)	11.70(-5.35)	31.68(+28.16)
Ours	<b>67.18(+18.83)</b>	<b>3.87(-1.47)</b>	<b>10.70(-5.24)</b>	<b>11.30(-5.75)</b>	26.70(+23.18)
Clean Training	70.13(+21.78)	2.83(-2.51)	10.94(-5.00)	11.07(-5.98)	100.00(+96.48)

**Note:** Values in parentheses denote changes relative to Noisy Training.  $\uparrow/\downarrow$  indicate that higher/lower values are better, respectively. **Bold** denotes the best performance in each column. **Budget** column denotes the sum of the crowd’s costs and correction costs and the pathologist’s costs. **Noisy Training** serves as the baseline, where the model is trained entirely on the uncleaned crowdsourced dataset  $D_c$ . **Ours (Random)** replaces the sample selection strategy in Step 1 with random selection, aiming to validate the effectiveness of the active learning approach. **Clean Training** refers to models fully supervised trained on the clean dataset  $D_p$ , which entirely annotated by pathologists.

In contrast, OA-MIL, which focuses on noise-robust learning without cleaning labels at the source, exhibits limited noise reduction efficacy and even increases Loc noise. Among label cleaning methods, Mao trained a cleaning model using noisy labels, but its performance was compromised by data noise, leading to inferior noise correction. In comparison, ALC, by incorporating active learning, it enhancing label cleaning effectiveness through pathologist involvement, outperforming Mao’s purely model-driven automatic correction, particularly for complex noise. Additionally, ALC’s active learning framework was not specifically designed for object detection tasks, limiting its performance, as also observed in Ours (Random). In summary, our proposed method achieves superior label correction quality while significantly reducing annotation cost—demonstrating a 73.30% reduction compared to Clean Training.

## 4.3 Qualitative Analysis of Noise Improvement

To visually assess the effectiveness of our proposed noise correction method, qualitative results are presented in Figure 5. The figure illustrates representative examples of various noise types before and after label correction. As shown in the first and second rows, our method successfully recovered several instances that were previously missed by the crowd (Miss). However, not all missing instances could be fully corrected, as indicated by the red arrow in Figure 5(e), which highlights a few labels still absent compared to pathologist annotations. In addition, the third and fourth rows demonstrate that our method effectively removed false positive labels on background regions (Bkg). Furthermore, the fifth and sixth rows show that the proposed method identified and corrected the bounding boxes that were either

misaligned or contained other boundaries (Loc and Bib). These visual results validate that our method can substantially improve annotation quality across multiple types of label noise.

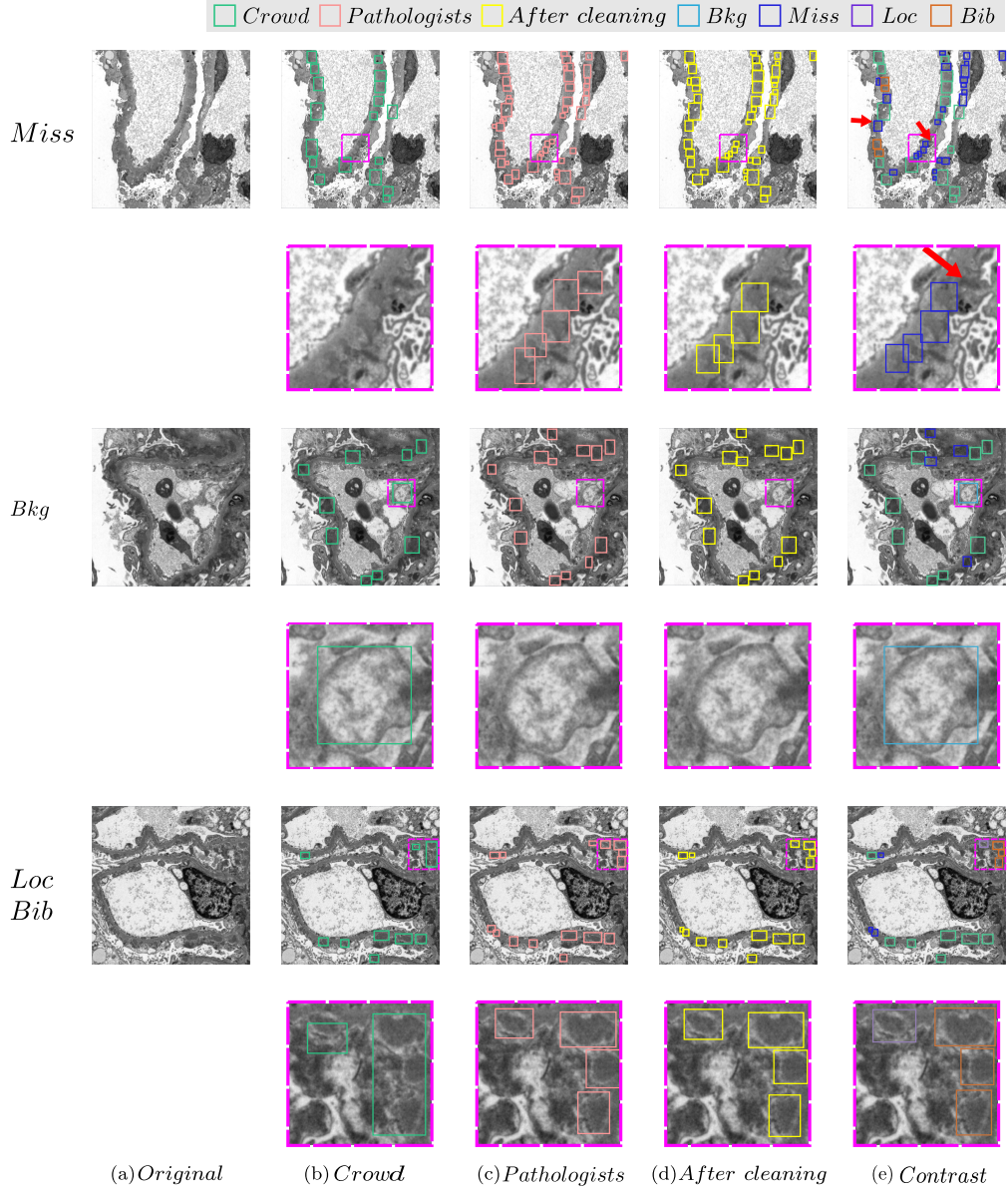


Figure 5: Qualitative results of label noise correction.

#### 4.4 Generalizability Study

To validate the generalization ability of the proposed method, we conducted experiments on the public BCCD dataset [27], comprising 205 training images, 87 validation images, and 72 test images. We simulated crowdsourced label by injecting Bkg, Miss, Loc and Bib noise into the training data at the same ratios as in the private dataset. As shown in Table 2, our method consistently achieved the best performance on the BCCD dataset, demonstrating an  $AP_{50}$  of 88.63%, a 4.81% improvement over the uncleaned baseline of Noisy Training, while significantly reducing all three noise types and reaching 97.97% of the Clean Training performance. Notably, the results revealed that OA-MIL outperformed Mao and ALC surpassed Ours(Random), which contrasts with the findings in Table 1. We attribute this difference to the BCCD dataset's limited scale, Mao's dependence on the amount of data, and the inherent high randomness in Ours (Random).

Table 2: Comparison of different noise treatment methods on public dataset.

Method	AP <sub>50</sub> (%)↑	TIDE Analysis			Budget(%)↓
		Bkg↓	Miss↓	Loc↓	
Noisy Training	83.82	10.15	0.77	2.42	3.43
OA-MIL	84.56(+0.74)	<b>5.25(-4.90)</b>	0.79(+0.02)	4.67(+2.25)	<b>3.43</b>
Mao	84.01(+0.19)	8.53(-1.62)	0.83(+0.06)	2.64(+0.22)	<b>3.43</b>
ALC	87.07(+3.25)	7.37(-2.78)	0.63(-0.14)	1.07(-1.35)	29.87(+26.44)
Ours (Random)	86.44(+2.62)	7.61(-2.54)	0.59(-0.18)	1.09(-1.33)	30.26(+26.83)
Ours	<b>88.63(+4.81)</b>	7.26(-2.89)	<b>0.57(-0.20)</b>	<b>0.69(-1.73)</b>	29.91(+26.48)
Clean Training	90.47(+6.65)	6.68(-3.47)	0.32(-0.45)	0.69(-1.73)	100.00(+96.57)

**Note:** Values in parentheses denote changes relative to Noisy Training. ↑/↓ indicate that higher/lower values are better, respectively. **Bold** denotes the best performance in each column. **Budget** column denotes the sum of the crowd’s costs and correction costs and the pathologist’s costs.

#### 4.5 Ablation Results

**The influence of active learning methods:** To evaluate the impact of different active learning methods on the performance of the two cleaning models,  $M_p$  and  $M_a$ , we compared our proposed approach with random selection (Random), task-unaware methods (VAAL and LLAL), classification-specific method (LC [28]), and detection-specific methods (LS+C, LT/C and CALD). As shown in Figure 6, all active learning methods outperformed Random, with the classification-specific method LC exhibiting inferior performance due to task mismatch. Moreover, detection-specific methods (LS+C, LT/C, CALD) and task-unaware approaches (VAAL, LLAL) achieved comparable results, likely because they were primarily designed for large-scale natural images and are less suitable for our small-scale dataset. In contrast, our method is specifically designed for EDD detection and demonstrates superior performance under limited data conditions. When the training samples increased to 200, our approach significantly surpassed all other methods in model accuracy, improving AP<sub>50</sub> by 6.80% for  $M_p$  and 6.70% for  $M_a$  compared to the Random.

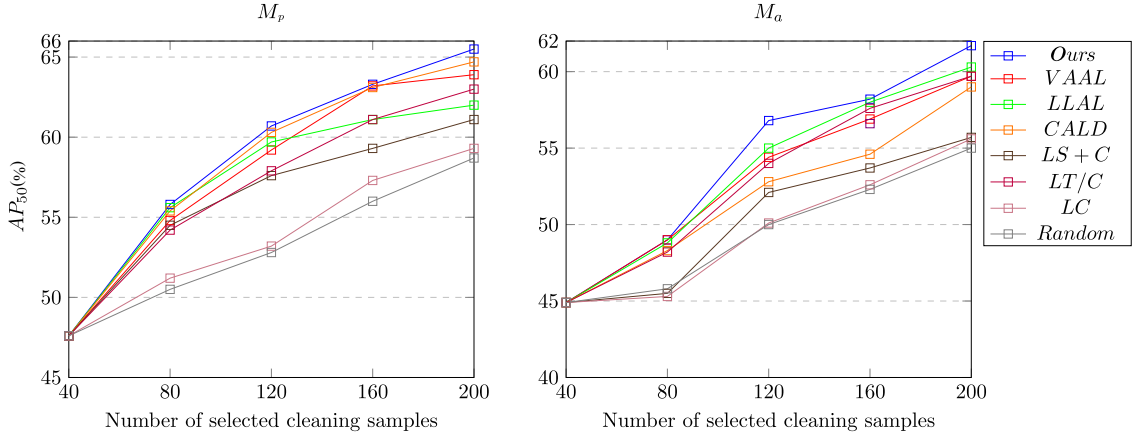


Figure 6: Influence of different Active Learning methods.

**The influence of Bib Correction Module:** We evaluated the impact of the Bib Correction Module on both label correction effectiveness and the time required for pathologists’ correction, while conducting an ablation study on the Bib noise threshold  $\gamma$  in Equation (3). As shown in Table 3, the introduction of the module successfully reduced the time pathologists spent on label corrections by about 10% without affecting the label correction effectiveness. Moreover, this improvement remained consistent across different threshold values of  $\gamma$ .

**The influence of  $M_a$  on sample selection and label correction:** To evaluate the effect of  $M_a$ , we compared the performance of the cleaning model  $M_p$  with and without the participation of  $M_a$ . As shown in Table 4, incorporating  $M_a$  improves the detection accuracy of  $M_p$  by 2.17%, enhancing the efficiency of sample selection. During the label

Table 3: Evaluating the impact of the Bib Correction Module on label correction time.

Bib module	$\gamma$	$AP_{50}(\%) \uparrow$	Time(%) $\downarrow$
$\times$	–	67.17	100.00
$\checkmark$	0.7	<b>67.18</b>	<b>90.37</b>
$\checkmark$	0.8	<b>67.18</b>	90.96
$\checkmark$	0.9	67.17	92.77

**Note:**  $\uparrow/\downarrow$  indicate that higher/lower values are better, respectively. **Bold** denotes the best performance in each column. **Time** is the ratio of pathologist’s label correction time when using the Bib Correction Module versus without it.

correction process, introducing  $M_a$  further improves accuracy by 3.88%. Moreover, combining the uncertainty of  $M_p$  and  $M_a$  significantly reduces Loc by 7.38% in the TIDE analysis, demonstrating the superior effectiveness of the dual-model collaboration.

Table 4: Evaluating the impact of the  $M_a$  model on sample selection and label correction.

$M_a$	$AP_{50}(\%) \uparrow$		TIDE Analysis		
	Cleaning Model	After Cleaning	Bkg $\downarrow$	Miss $\downarrow$	Loc $\downarrow$
$\times$	63.33	63.30	22.28	12.85	19.13
$\checkmark$	<b>65.50(+2.17)</b>	<b>67.18(+3.88)</b>	22.16(-0.12)	12.65(-0.20)	<b>11.75(-7.38)</b>

**Note:** Values in parentheses denote changes relative to the baseline ( $M_a=\times$ ).  $\uparrow/\downarrow$  indicate that higher/lower values are better, respectively. **Bold** denotes the best performance in each column.

## 5 Conclusions

We propose an active label cleaning method for addressing label noise in crowdsourced label for EDD detection, which balances performance and cost. Specifically, we employ active learning to select the most valuable samples, constructing the high-accuracy cleaning models with minimal pathologist’s annotation. Subsequently, we implement noise-graded correction to reduce annotation cost without compromising label correction quality. The designed Label Selection Module analyzes the inconsistency between the crowdsourced labels and the model predictions to achieve image-level sample selection and instance-level noise grading, serving as an effective auxiliary tool. Finally, experimental results demonstrate that the proposed method achieves optimal results on both private and public datasets, confirming its effectiveness and generalizability.

## Author contributions

Conceptualization, J.T.; methodology, J.T. and S.L.; software, J.T. and S.L.; validation, J.T. and S.L.; data curation, J.G.; writing—original draft preparation, J.T.; writing—review and editing, J.T., S.L., G.Z., Z.L., L.Z. and L.C.; supervision, L.C.; funding acquisition, L.Z. and L.C. All authors have read and agreed to the published version of the manuscript.

## Acknowledgments

This research was funded by the grant from the National Natural Science Foundation of China (No. 32071368), the Guangdong Basic and Applied Basic Research Foundation (No. 2022A1515110162) and the Clinical Research Fund of Nanfang Hospital, Southern Medical University (No. 2023CR024).

## Financial disclosure

None reported.

## Conflict of interest

The authors declare no potential conflict of interests.

## Data Availability Statement

The datasets analyzed during the current study are not publicly available due to patient confidentiality and privacy restrictions but are available from the corresponding author on reasonable request.

## Ethics approval statement

The study was conducted in accordance with the Declaration of Helsinki, and approved by the Ethics Committee of Medical Ethics Committee of Nanfang Hospital of Southern Medical University (NFEC-2024-328 and 1 July 2024).

## References

- [1] David Kipgen and Colin Geddes. Diagnostic and prognostic significance of extent of subepithelial electron dense deposits in membranous glomerulonephritis. *Ultrastructural Pathology*, 45(3):224–235, 2021.
- [2] Jingyuan Zhang and Aihua Zhang. Deep learning-based multi-model approach on electron microscopy image of renal biopsy classification. *BMC nephrology*, 24(1):132, 2023.
- [3] Anran Liu, Xiangsheng Huang, Tong Li, and Pengcheng Ma. Co-net: A collaborative region-contour-driven network for fine-to-finer medical image segmentation. In *Proceedings of the IEEE/CVF Winter Conference on Applications of Computer Vision*, pages 1046–1055, 2022.
- [4] Shuo Liu, Jieyun Tan, Yanmeng Lu, Jian Geng, Zhitao Zhou, and Lei Cao. Deformable r-cnn for detection of electron dense deposits in glomerular transmission electron microscopy images. *IEEE Access*, 12:25657–25667, 2024.
- [5] Shanshan Wang, Cheng Li, Rongpin Wang, Zaiyi Liu, Meiyun Wang, Hongna Tan, Yaping Wu, Xinfeng Liu, Hui Sun, Rui Yang, et al. Annotation-efficient deep learning for automatic medical image segmentation. *Nature communications*, 12(1):5915, 2021.
- [6] Silas Ørting, Andrew Doyle, Arno van Hiltén, Matthias Hirth, Oana Inel, Christopher R Madan, Panagiotis Mavridis, Helen Spiers, and Veronika Cheplygina. A survey of crowdsourcing in medical image analysis. *arXiv preprint arXiv:1902.09159*, 2019.
- [7] Bryce Nicholson, Victor S Sheng, and Jing Zhang. Label noise correction and application in crowdsourcing. *Expert Systems with Applications*, 66:149–162, 2016.
- [8] Davood Karimi, Haoran Dou, Simon K Warfield, and Ali Gholipour. Deep learning with noisy labels: Exploring techniques and remedies in medical image analysis. *Medical image analysis*, 65:101759, 2020.
- [9] Jiyang Gao, Jiang Wang, Shengyang Dai, Li-Jia Li, and Ram Nevatia. Note-rcnn: Noise tolerant ensemble rcnn for semi-supervised object detection. In *Proceedings of the IEEE/CVF international conference on computer vision*, pages 9508–9517, 2019.
- [10] Chengxin Liu, Kewei Wang, Hao Lu, Zhiguo Cao, and Ziming Zhang. Robust object detection with inaccurate bounding boxes. In *European Conference on Computer Vision*, pages 53–69. Springer, 2022.
- [11] Junnan Li, Caiming Xiong, Richard Socher, and Steven Hoi. Towards noise-resistant object detection with noisy annotations. *arXiv preprint arXiv:2003.01285*, 2020.
- [12] Jiafeng Mao, Qing Yu, and Kiyoharu Aizawa. Noisy localization annotation refinement for object detection. *IEICE TRANSACTIONS on Information and Systems*, 104(9):1478–1485, 2021.
- [13] Mélanie Bernhardt, Daniel C Castro, Ryutaro Tanno, Anton Schwaighofer, Kerem C Tezcan, Miguel Monteiro, Shruthi Bannur, Matthew P Lungren, Aditya Nori, Ben Glocker, et al. Active label cleaning for improved dataset quality under resource constraints. *Nature communications*, 13(1):1161, 2022.
- [14] Jan Schneegans, Maarten Bieshaar, and Bernhard Sick. A practical evaluation of active learning approaches for object detection. In *IAL@ PKDD/ECML*, pages 49–67, 2022.
- [15] Haoran Wang, Qiuye Jin, Shiman Li, Siyu Liu, Manning Wang, and Zhijian Song. A comprehensive survey on deep active learning in medical image analysis. *Medical Image Analysis*, page 103201, 2024.

- [16] Ümit Mert Çağlar, Alperen İnci, Oğuz Hanoglu, Görkem Polat, and Alptekin Temizel. Ulcerative colitis mayo endoscopic scoring classification with active learning and generative data augmentation. In *2023 IEEE International Conference on Bioinformatics and Biomedicine (BIBM)*, pages 462–467. IEEE, 2023.
- [17] Chieh-Chi Kao, Teng-Yok Lee, Pradeep Sen, and Ming-Yu Liu. Localization-aware active learning for object detection. In *Computer Vision–ACCV 2018: 14th Asian Conference on Computer Vision, Perth, Australia, December 2–6, 2018, Revised Selected Papers, Part VI 14*, pages 506–522. Springer, 2019.
- [18] Weiping Yu, Sijie Zhu, Taojiannan Yang, and Chen Chen. Consistency-based active learning for object detection. In *Proceedings of the IEEE/CVF conference on computer vision and pattern recognition*, pages 3951–3960, 2022.
- [19] Jiao Tang, Yagao Yue, Peng Wan, Mingliang Wang, Daoqiang Zhang, and Wei Shao. Osal-nd: Open-set active learning for nucleus detection. In *International Conference on Medical Image Computing and Computer-Assisted Intervention*, pages 351–361. Springer, 2024.
- [20] Samarth Sinha, Sayna Ebrahimi, and Trevor Darrell. Variational adversarial active learning. In *Proceedings of the IEEE/CVF international conference on computer vision*, pages 5972–5981, 2019.
- [21] Donggeun Yoo and In So Kweon. Learning loss for active learning. In *Proceedings of the IEEE/CVF conference on computer vision and pattern recognition*, pages 93–102, 2019.
- [22] Bidur Khanal, Tianhong Dai, Binod Bhattacharai, and Cristian Linte. Active label refinement for robust training of imbalanced medical image classification tasks in the presence of high label noise. In *International Conference on Medical Image Computing and Computer-Assisted Intervention*, pages 37–47. Springer, 2024.
- [23] Huy V Vo, Oriane Siméoni, Spyros Gidaris, Andrei Bursuc, Patrick Pérez, and Jean Ponce. Active learning strategies for weakly-supervised object detection. In *European conference on computer vision*, pages 211–230. Springer, 2022.
- [24] Kai Chen, Jiaqi Wang, Jiangmiao Pang, Yuhang Cao, Yu Xiong, Xiaoxiao Li, Shuyang Sun, Wansen Feng, Ziwei Liu, Jiarui Xu, et al. Mmdetection: Open mmlab detection toolbox and benchmark. *arXiv preprint arXiv:1906.07155*, 2019.
- [25] Shaoqing Ren, Kaiming He, Ross Girshick, and Jian Sun. Faster r-cnn: Towards real-time object detection with region proposal networks. *Advances in neural information processing systems*, 28, 2015.
- [26] Daniel Bolya, Sean Foley, James Hays, and Judy Hoffman. Tide: A general toolbox for identifying object detection errors. In *Computer Vision–ECCV 2020: 16th European Conference, Glasgow, UK, August 23–28, 2020, Proceedings, Part III 16*, pages 558–573. Springer, 2020.
- [27] Partha Pratim Banik, Rappy Saha, and Ki-Doo Kim. An automatic nucleus segmentation and cnn model based classification method of white blood cell. *Expert Systems with Applications*, 149:113211, 2020.
- [28] Samuel Budd, Emma C Robinson, and Bernhard Kainz. A survey on active learning and human-in-the-loop deep learning for medical image analysis. *Medical image analysis*, 71:102062, 2021.